

**DOCUMENT**

|                     |                 |             |            |
|---------------------|-----------------|-------------|------------|
| Deliverable Number  | <b>D3.1</b>     | Due Date    | 31/01/2015 |
| Issued by WP/Task   | <b>WP3/T3.1</b> | Actual Date | 31/01/2015 |
| Dissemination Level | <b>PUBLIC</b>   | Pages       | 34         |
|                     |                 | Appendices  | none       |

**PROJECT**

|                     |  |
|---------------------|--|
| Grant Agreement No. | 606645   |
| Acronym             | RPB HealTec  |
| Title               | ROAD PAVEMENTS & BRIDGE DECK HEALTH MONITORING /<br>EARLY WARNING USING ADVANCED INSPECTION TECHNOLOGIES |
| Call                | <b>FP7-SME-2013</b>  |
| Funding Scheme      | BSG-SME  |

## **Deliverable D3.1**

### **Thermography procedures – guidelines and essential parameters for Thermography (modelling)**

**AUTHORS**

|                   |                           |
|-------------------|---------------------------|
| CERTH             | S. MOUSTAKIDIS            |
| IRIS-Thermovision | M. HOVENS                 |
| CITY              | P. LIATIS, A.UUS, P. SHAW |

**APPROVAL**

|                       |       |                |
|-----------------------|-------|----------------|
| Workpackage Leader    | CERTH | S. MOUSTAKIDIS |
| Technical Coordinator | CERTH | S. MOUSTAKIDIS |
| Project Coordinator   | CITY  | P. LIATIS      |

**AUTHORIZATION**

|                 |     |                |
|-----------------|-----|----------------|
| Project Officer | REA | K. AMOLOCHITIS |
|-----------------|-----|----------------|



## CONSORTIUM

---

|   | <b>Beneficiary name</b>                                   | <b>Country</b> |
|---|---|----------------|
| 1 | City University London (CITY)                             | UK             |
| 2 | I&T Nardoni Institute S.R.L. (NARDONI)                    | Italy          |
| 3 | MET GEOENVIRONMENTAL (METGEO)                             | UK             |
| 4 | Global Digital Technologies (GDT)                         | Greece         |
| 5 | IRIS Thermovision (IRIS)                                  | Netherlands    |
| 6 | Autostrada del Brennero SpA Brennerautobahn AG (BRENNERO) | Italy          |
| 7 | Vrancea County Council (CJ VRANCEA)                       | Romania        |
| 8 | CENTER FOR RESEARCH & TECHNOLOGY HELLAS (CERTH)           | Greece         |
| 9 | Center for Research Technology & Innovation (CETRI)       | Cyprus         |

**REVISION HISTORY**

---

| <b>VER.</b> | <b>DATE</b> | <b>PAGES</b> | <b>NOTES</b>   | <b>AUTHORS (partners)</b>  |
|-------------|-------------|--------------|--|--|
| 01          | 10/11/2014  | All          | First draft (structure)  | P. Liatsis (CITY), S. Moustakidis (CERTH)                                |
| 02          | 10/12/2014  | All          | Input requirements from the end users                                  | I. de Biasi (BRENNERO), D. Olaru (CJ VRANCEA)                            |
| 03          | 15/12/2014  | All          | Experimental results   | S. Moustakidis (CERTH)   |
| 04          | 15/01/2015  | All          | Second draft submitted to SMEs   | M. Hovens (IRIS), S. Twist (METGEO), G. Nardoni (NARDONI)                |
| 05          | 20/01/2015  | All          | Technical review   | A. Uus (CITY), P. Shaw (CITY), G. Doumenis (GDT)                         |
| 06          | 28/01/2015  | All          | Corrections incorporated   | S. Moustakidis (CERTH)   |
| 07          | 30/01/2015  | All          | Final draft with input from Coordinator and comments from the partners | S. Moustakidis (CERTH), P. Liatsis (CITY), A. Uus (CITY), P. Shaw (CITY) |
| Final       | 31/01/2015  | All          | Approved   | P. Liatsis (CITY)  |



## **EXECUTIVE SUMMARY**

---

WP3 is concerned with the development of an advanced IR thermography system for detection of defects in pavement structures. In the context of the WP, D3.1 aims to investigate, through simulation studies, the development of the proposed sensing system and the associated procedures for calibration and setup.

It commences with a brief introduction to heat transfer analysis, which is followed by the 3D FEM models and associated details and assumptions, developed for the purposes of investigating defects in pavements. Next, detailed studies in terms of the thermal response of the delaminations for each of the associated case studies are presented, focusing on the temperature differential (TD), and its relationship with the depth of the defect, presence of moisture and exposure times.



## TABLE OF CONTENTS

---

|     |  |    |
|-----|--|----|
| 1   | INTRODUCTION .....   | 7  |
| 2   | HEAT TRANSFER ANALYSIS .....   | 8  |
| 3   | FINITE ELEMENT MODELING.....   | 9  |
| 4   | RESULTS AND DUSCUSSION .....   | 12 |
| 4.1 | Intact asphalt.....  | 12 |
| 4.2 | Asphalt with dry (air) or wet (water) debonded layer at 5cm depth..... | 14 |
| 4.3 | Asphalt with dry (air) or wet (water) debonded layer at 1cm depth..... | 18 |
| 4.4 | Asphalt with partially debonded layer at 1cm depth .....               | 22 |
| 4.5 | Asphalt with dry (air) or wet (water) stripped layer at 5cm depth..... | 27 |
| 4.6 | Effect of asphalt thermal conductivity.....                            | 29 |
| 5   | CONCLUSIONS .....  | 33 |
| 6   | REFERENCES .....   | 34 |



## ABBREVIATIONS

---

|      |   |
|------|---|
| FE   | Finite Element                            |
| MRTD | Minimum Resolvable Temperature Difference |
| TD   | Temperature Differential                  |
| EUs  | End Users                                 |
| IRT  | Infrared Thermography                     |
| NDT  | Non-Destructive Testing                   |
| REA  | Research Executive Agency                 |
| WP   | Work Package                              |

## 1 INTRODUCTION

This report is concerned with the thermal behavior of intact and defective asphalt pavements subjected to solar heat loads. Three dimensional Finite Element (FE) models are developed in order to simulate and compare simulation results between defective and non-defective pavements during a thermography process. The simulation results are used to examine the ability of subsurface defect detection by thermography processes and support the laboratory and field evaluations. The pavement layer design and condition, as well as environmental conditions are taken into account in the current analyses.

The pavement structure considered for the analyses has dimensions 60mm x 60mm x 200mm (length x width x depth). The pavement contained subsurface defects of varying sizes at various depths. Heat transfer analyses were conducted on the 3D structure at different environmental conditions in order to investigate the thermal response of the defective pavement and determine the capability of capturing the defects by thermographic techniques. The 3D geometric representation of the model used in the analyses is shown in Figure 1.

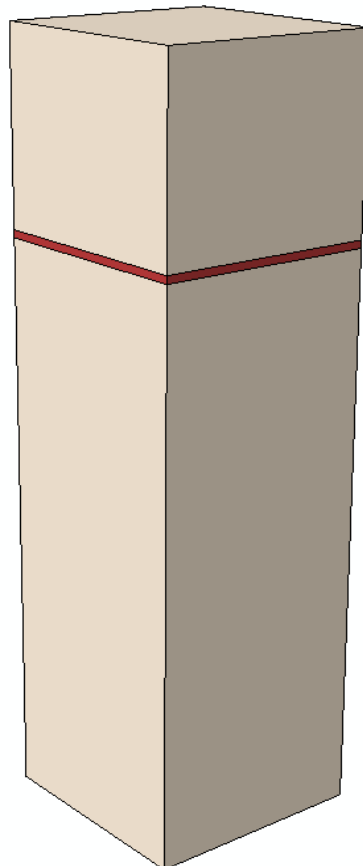


*Figure 1: Schematic representation of the 3D structure of dimensions 60mm x 60mm x 200mm (length x width x depth) containing a defective layer of thickness 2mm at 50mm depth.*

## 2 HEAT TRANSFER ANALYSIS

In this section we present the mathematical formulation of the heat transfer analysis. The following formulation applies to homogeneous isotropic solid body heat conduction with convection and radiation boundary conditions. The energy balance is given by

$$\int_V \rho U \dot{d}V = \int_S -\mathbf{q} \cdot \mathbf{n} dS \quad \forall V \quad \Rightarrow$$

$$\rho U \dot{+} \nabla \cdot \mathbf{q} = 0 \quad (1)$$

where  $V$  is a volume occupied by a solid material bounded by a surface  $S$ ,  $\rho$  is the mass density of the material ( $\text{Kg}/\text{m}^3$ ),  $U$  is the internal energy per unit mass ( $\text{J}/\text{Kg}$ ),  $\mathbf{q}$  is the heat flux per unit area ( $\text{W}/\text{m}^2$ ),  $\mathbf{n}$  is the outward unit normal on the body surface, and a superposed dot denotes the material time derivative. Equation (1) is usually written in terms of specific heat  $c(T) = \frac{\partial U(T)}{\partial T}$  ( $\text{J}/\text{Kg } ^\circ\text{C}$ ) where  $T$  is temperature, so that

$$U \dot{=} \frac{\partial U(T)}{\partial T} T \dot{=} c T \dot{=} \quad (2)$$

Heat conduction is assumed to be governed by the isotropic Fourier law:

$$\mathbf{q} = -\mathbf{k} \cdot \nabla T \quad (3)$$

where  $\mathbf{k}$  is the thermal conductivity tensor ( $\text{W}/\text{m } ^\circ\text{C}$ ). Combining equations (1), (2), and (3) we arrive at the governing equation for transient heat transfer analysis:

$$\nabla \cdot (\mathbf{k} \cdot \nabla T) = \rho c T \dot{=} \quad (4)$$

Heat losses due to convection and radiation are specified as boundary conditions:

$$\mathbf{q} \cdot \mathbf{n} = h(T - T_0) + \sigma \varepsilon \left[ (T - T_z)^4 - (T_0 - T_z)^4 \right] \quad (5)$$

where  $h$  is the film coefficient ( $\text{W}/\text{m}^2 \text{ } ^\circ\text{C}$ ),  $T_0$  is the sink temperature,  $T_z$  is the absolute zero temperature,  $\varepsilon$  is the emissivity (dimensionless), and  $\sigma = 5.67 \times 10^{-8} \text{W}/\text{m}^2 \text{ } ^\circ\text{C}^4$  is the Stefan-Boltzmann constant.

### 3 FINITE ELEMENT MODELING

3D models were created based on the geometrical characteristics of the pavement structure considered for analysis in the current study. All FE modeling and analyses were carried out using the ABAQUS v6.12 general purpose finite element program [1]. Several cases were considered for analysis:

- a) pavement with a debonded layer of thickness 2mm at 50mm depth (Figure 2a)
- b) pavement with a debonded layer of thickness 2mm at 10mm depth (Figure 2b)
- c) pavement with a stripped layer of thickness 20mm at 50mm depth (Figure 2c)
- d)

The finite element meshes of the 3D structures presented in Figure 2 are shown in Figure 3. A finer mesh is used around the delamination region and the stripped layer in order to capture accurately the temperature gradients in these regions. The debonded layer and the stripped layer are meshed with five (5) and ten (10) elements through the thickness respectively. The 3D models of pavement containing a debonded layer consist of about 79,000 nodes and 86,000 8-node diffusive heat transfer linear brick elements. The 3D models of pavement containing a stripped layer consist of about 38,500 nodes and 42,500 8-node diffusive heat transfer linear brick elements. In both model cases, mesh sensitivity studies were carried out to ensure convergent numerical calculation of temperature.

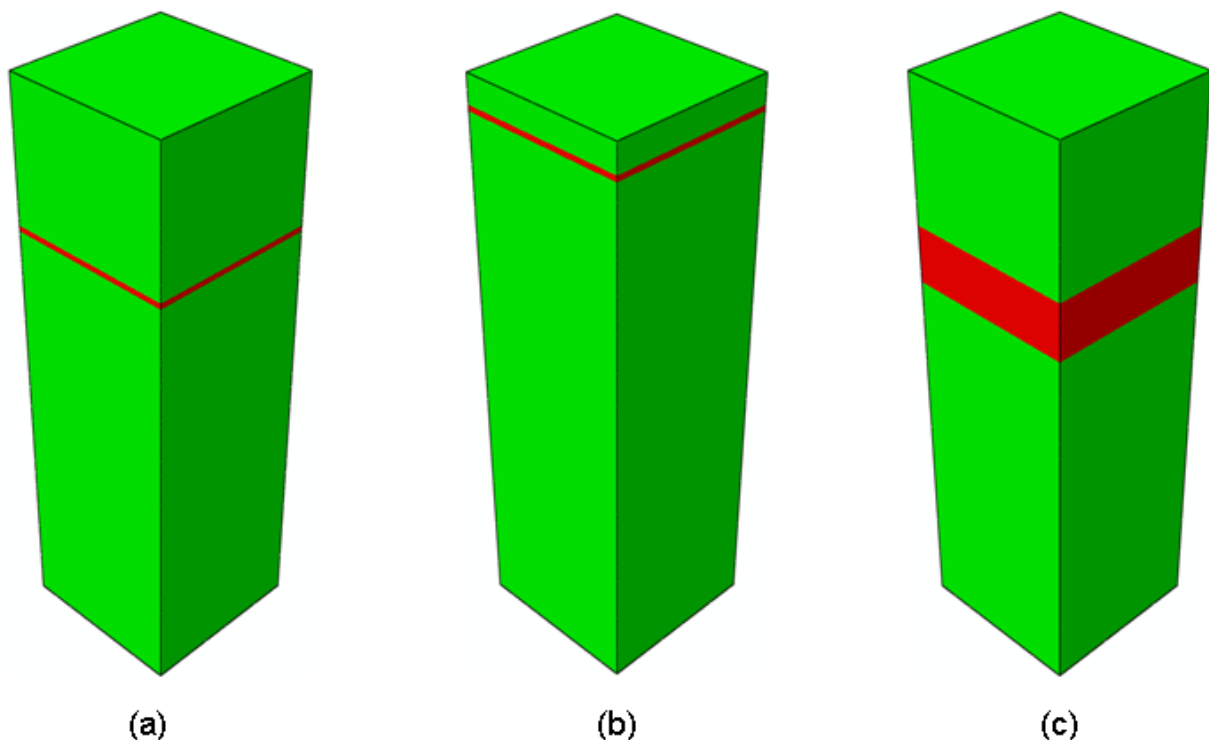


*Figure 2: Model representation of the 3D pavement structure containing: a) debonded layer of thickness 2mm at 50mm depth, b) debonded layer of thickness 2mm at 10mm depth, c) stripped layer of thickness 20mm at 50mm depth.*

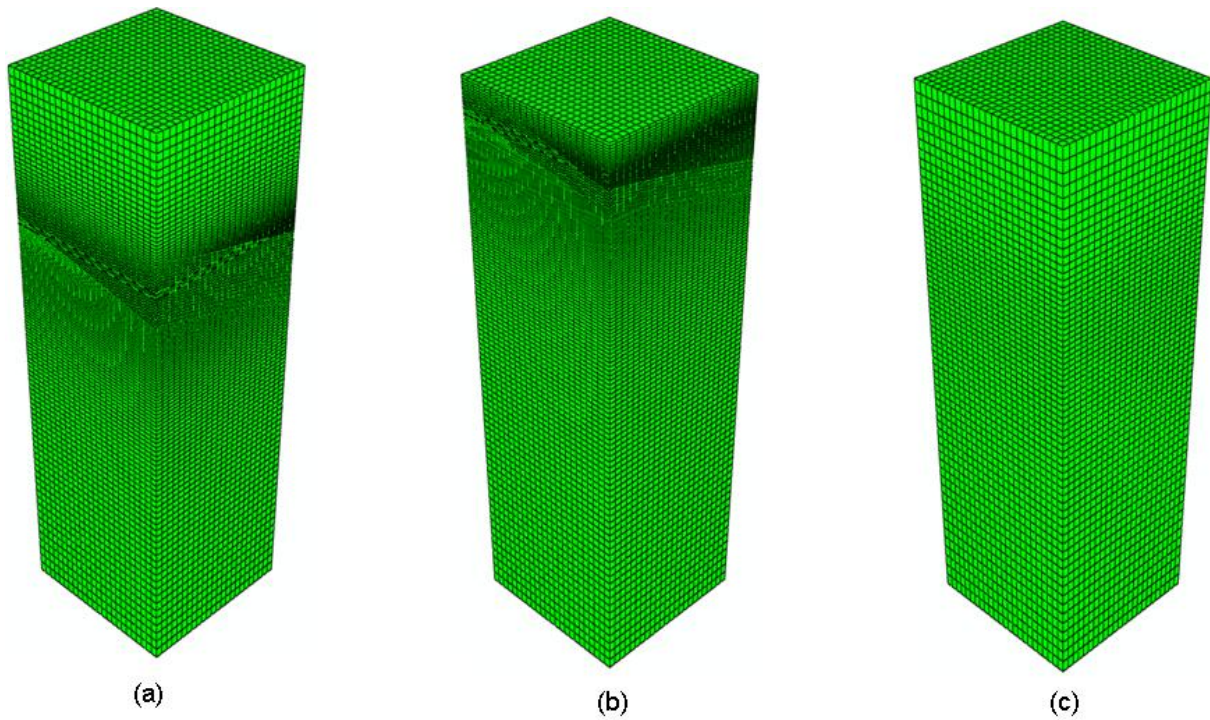


Figure 3: FE meshes of the 3D pavement structures containing: a) debonded layer of thickness 2mm at 50mm depth, b) debonded layer of thickness 2mm at 10mm depth, c) stripped layer of thickness 20mm at 50mm depth.

The pavement material (asphalt) is considered to be homogeneous and isotropic. The temperature range that the pavement can reach under normal weather conditions is between about 0°C and 50°C. In this temperature range, the values of material thermal properties do not change significantly and thus the temperature-dependence of material properties can be neglected in the current problem. The material properties used in the current analyses for asphalt and the defective regions are summarized in Table 1 [2].

Table 1: Thermo-physical properties for the materials used in the FE analyses.

| Material                           | Density<br>(Kg / m <sup>3</sup> ) | Thermal Capacity<br>(J/Kg · K) | Thermal<br>Conductivity<br>(W / m · K) |
|------------------------------------|-----------------------------------|--------------------------------|--|
| Intact Asphalt                     | 2300                              | 1100                           | 1                                      |
| Stripped Asphalt                   | 1800                              | 1100                           | 0.75                                   |
| Stripped Asphalt<br>with 10% water | 2170                              | 1408                           | 0.95                                   |
| Air at 25°C                        | 1.2                               | 1006                           | 0.026                                  |
| Water at 25°C                      | 1000                              | 4186                           | 0.6                                    |

Based on the formulation described in Section 2 heat transfer analyses for intact and defective pavement are carried out. A thermal flux equal to the solar heat load is applied uniformly on the surface of the structure. The heat flux magnitude and distribution are dependent on the environmental conditions. Figure 4 shows a typical daily distribution of solar flux on a flat surface during summer, spring/autumn, and winter periods which are used in the analyses.

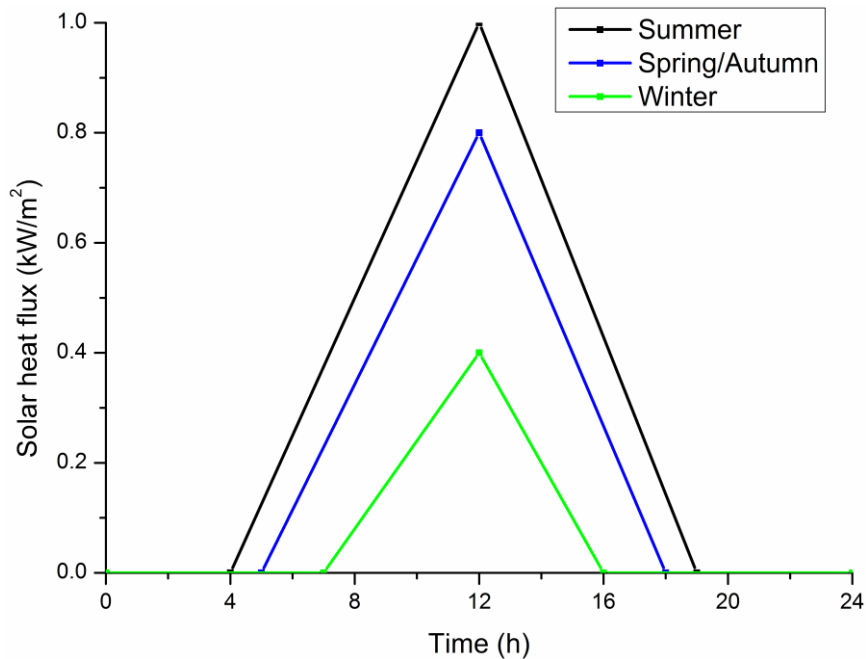


Figure 4: Typical daily distribution of solar flux on a flat surface during summer, spring/autumn, and winter periods.

The surface of the pavement experiences also heat losses due to free air convection and radiation with film coefficient  $h = 20 \text{ W/m}^2 \text{ }^\circ\text{C}$  and emissivity  $\varepsilon = 0.7$  [3]. The ambient temperature is considered to depend on the season; the values used in the analyses are summarized in Table 2 based on measurements presented in Deliverable D1.2 “Preliminary design and selection of appropriate sites for damage assessment and/or inspection” [4]. Symmetry boundary conditions are considered at the side surfaces of the models; the side surfaces are considered to be adiabatic. Also, the bottom surface is considered insulated.

Table 2: Ambient temperature used in the analyses

| Season        | Ambient Temperature ( $^\circ\text{C}$ ) |
|---------------|--|
| Summer        | 20                                       |
| Spring/Autumn | 10                                       |
| Winter        | 2  |

## 4 RESULTS AND DUSCUSSION

The temperature developed at the surface of intact and defective pavement during a day cycle was numerically obtained for analysing the thermal response of delaminations. The analysis of the thermal response of delaminations is based on the computation of the temperature differential (TD), which is the difference between the temperature on the surface of the defective structure and the temperature on the surface of the intact structure. It is noted that the Minimum Resolvable Temperature Difference (MRTD) for the most of the available thermal imager (IR camera) is around  $0.1^{\circ}\text{C}$  [5] which is chosen as a threshold value for the current analyses to investigate/identify the delaminations in pavement structures.

First, the thermal response of the intact asphalt pavement is studied. Then, the 3D models are used to study the effects of dry and wet delaminations at various depths on the temperature differential produced on the pavement surface.

### 4.1 Intact asphalt

The temperature distribution through the thickness of the intact asphalt pavement and the temporal variation of temperature during a day cycle for three seasonal periods (summer, autumn/spring, winter) are presented in this section. The whole structure is assumed to be made of intact asphalt with properties given in Table 1. In Figure 5 temperature contours at the intact pavement structure during autumn/spring period at the time of maximum surface temperature are presented. The results in Figure 5 indicate that the maximum temperature appears at the pavement surface and that the temperature is decreased as getting deeper in the structure. Figure 6 shows the daily variation of temperature at the pavement surface for different seasonal periods. As expected, the temperature distribution in all cases follows the solar heat flux distribution shown in Figure 4. The maximum temperature appears at 12 o'clock noon and a value of  $48^{\circ}\text{C}$  in summer periods,  $32^{\circ}\text{C}$  in autumn/spring periods and  $12^{\circ}\text{C}$  in winter periods is calculated.

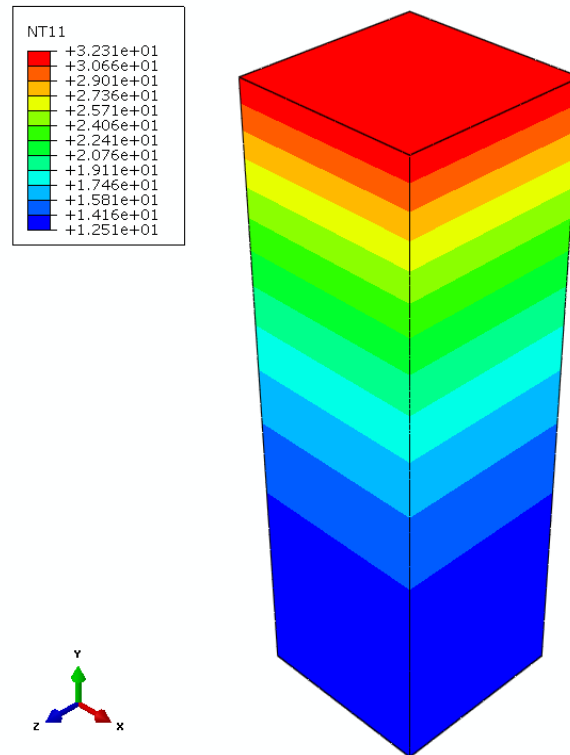


Figure 5: Temperature distribution of *intact asphalt* pavement during spring/autumn period at time of maximum surface temperature.

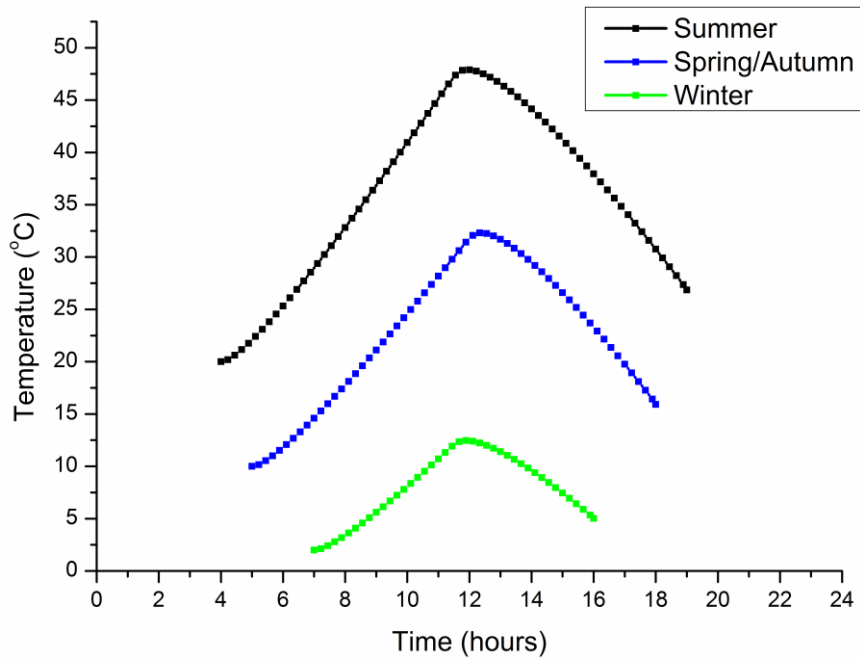


Figure 6: Daily variation of temperature at the surface of *intact asphalt* pavement during summer, spring/autumn, and winter periods.

#### 4.2 Asphalt with dry (air) or wet (water) debonded layer at 5cm depth

In this section, the effect of dry and wet debonded layers of thickness 2mm located at 5cm depth on the temperature differential produced on the pavement surface is examined. The dry layer is filled with air whereas the wet layer is filled with water; the properties for air and water are shown in Table 1. The rest pavement structure is assumed to be made of intact asphalt.

Figures 7, 8, and 9 show the daily variation of temperature differential TD at the pavement surface between the non-defective structure and the structure with air-filled or water-filled debonded layer located at 5cm depth during summer period, spring/autumn period, winter period respectively. In all cases maximum TD appears around 13 o'clock noon and a value of about 2°C in summer periods, 1.7°C in autumn/spring periods and 0.9°C in winter periods is calculated. The results show that during all periods sufficient TD is developed on the pavement surface in order for the air-filled debonded layer to be detected during a thermography process. On the other hand, the water-filled debonded layer produces insignificant TD and thus may not be detected by a thermal imager.

Figure 10 shows the daily variation of TD at the pavement surface between the non-defective structure and the structure with air-filled debonded layer located at 5cm depth for all the seasonal periods together. The results indicate that the highest and lowest TD are developed during summer and winter periods respectively. A temperature differential more close to that developed during summer periods is developed during spring/autumn periods.

Figures 11, 12, and 13 show the daily variation of temperature at the pavement surface for intact asphalt and asphalt with the air-filled debonded layer during summer period, spring/autumn period, winter period respectively. TD is defined as the difference between the temperature developed on the defective structure and the temperature on the intact structure.

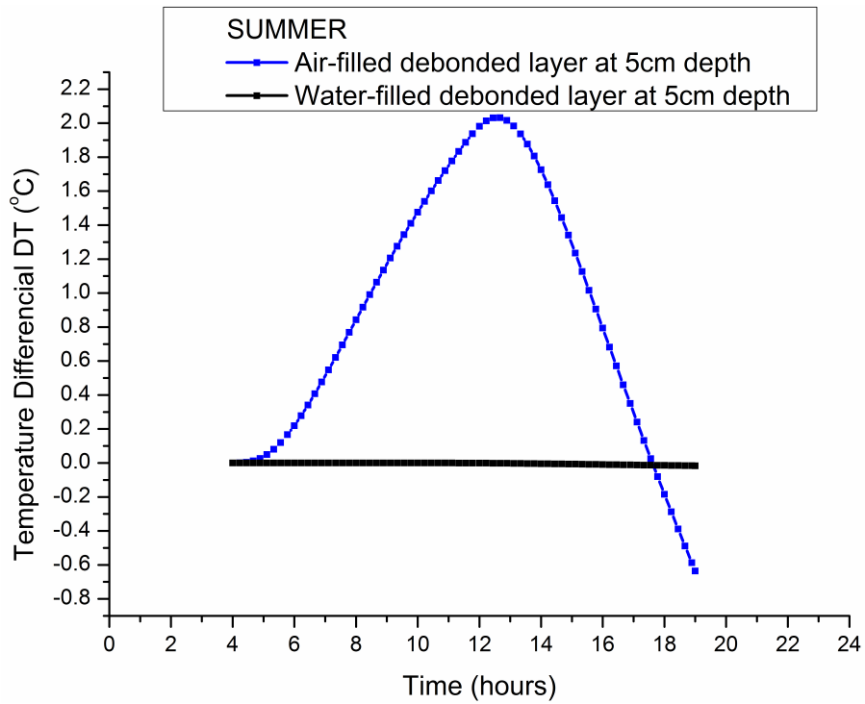


Figure 7: Daily variation of TD at the pavement surface between the non-defective structure and the structure with air-filled and water-filled debonded layer located at 5cm depth during summer period.

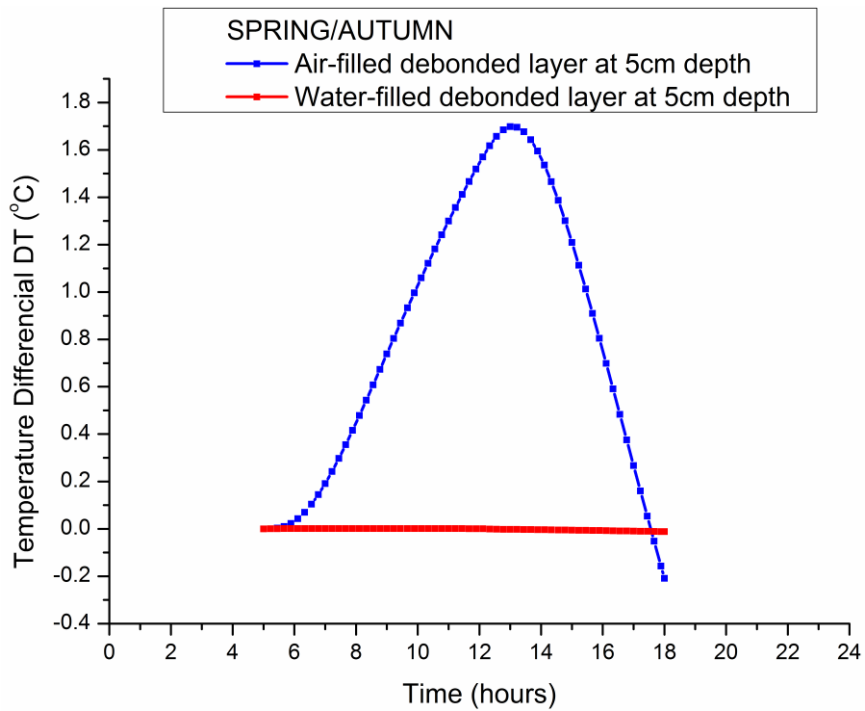


Figure 8: Daily variation of TD at the pavement surface between the non-defective structure and the structure with air-filled and water-filled debonded layer located at 5cm depth during spring/autumn period.

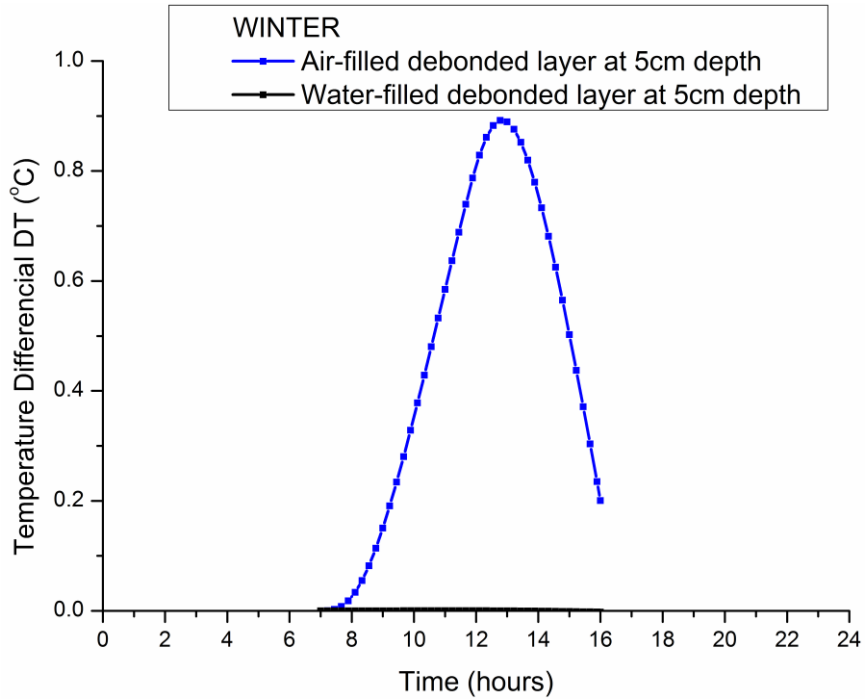


Figure 9: Daily variation of TD at the pavement surface between the non-defective structure and the structure with air-filled and water-filled debonded layer located at 5cm depth during winter period.

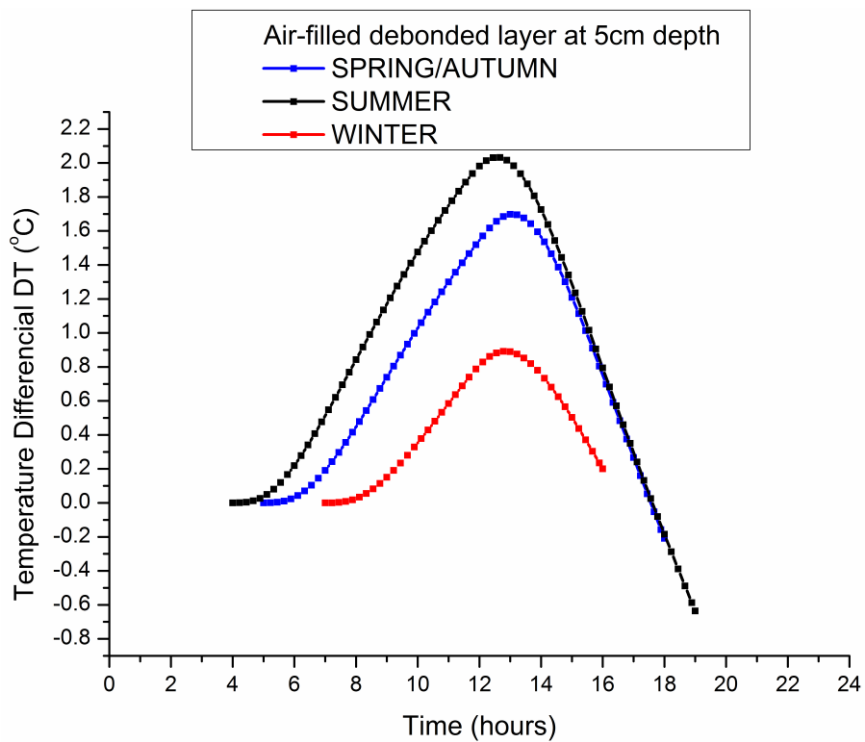


Figure 10: Daily variation of TD at the pavement surface between the non-defective structure and the structure with air-filled debonded layer located at 5cm depth.

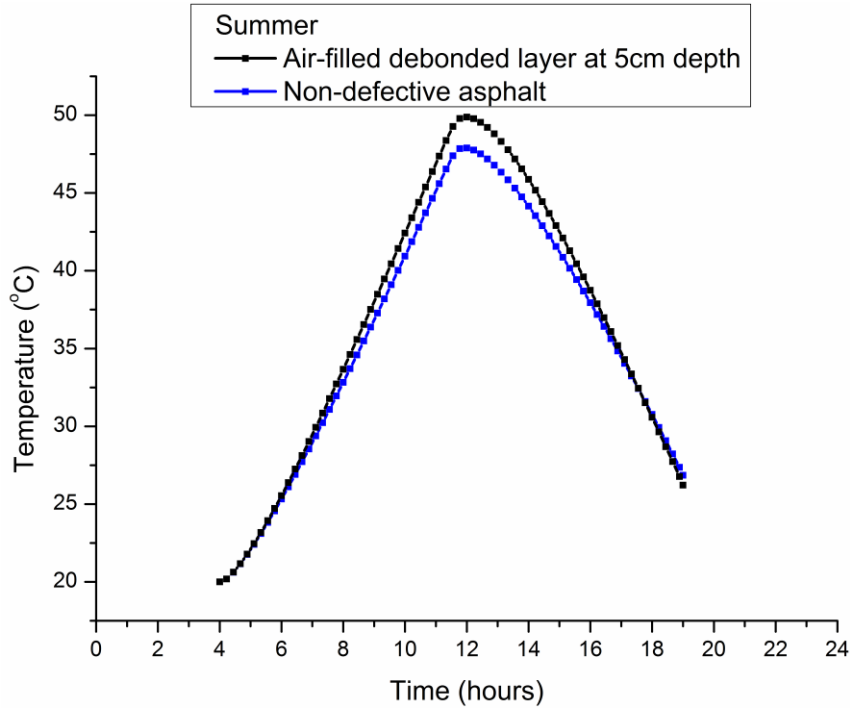


Figure 11: Daily temperature variation at the pavement surface between the non-defective structure and the structure with air-filled debonded layer located at 5cm depth during summer period.

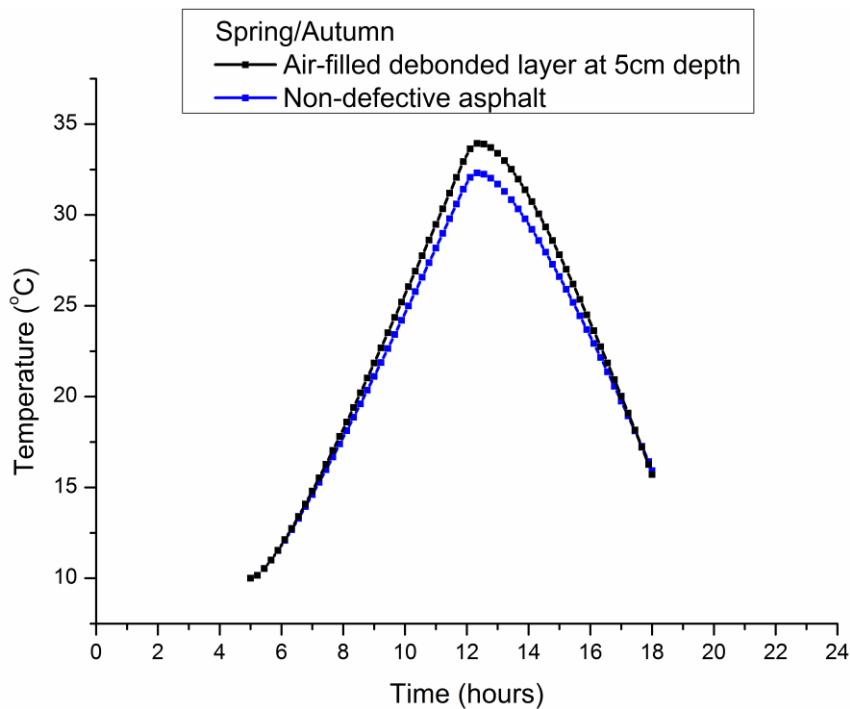


Figure 12: Daily temperature variation at the pavement surface between the non-defective structure and the structure with air-filled debonded layer located at 5cm depth during spring/autumn period.

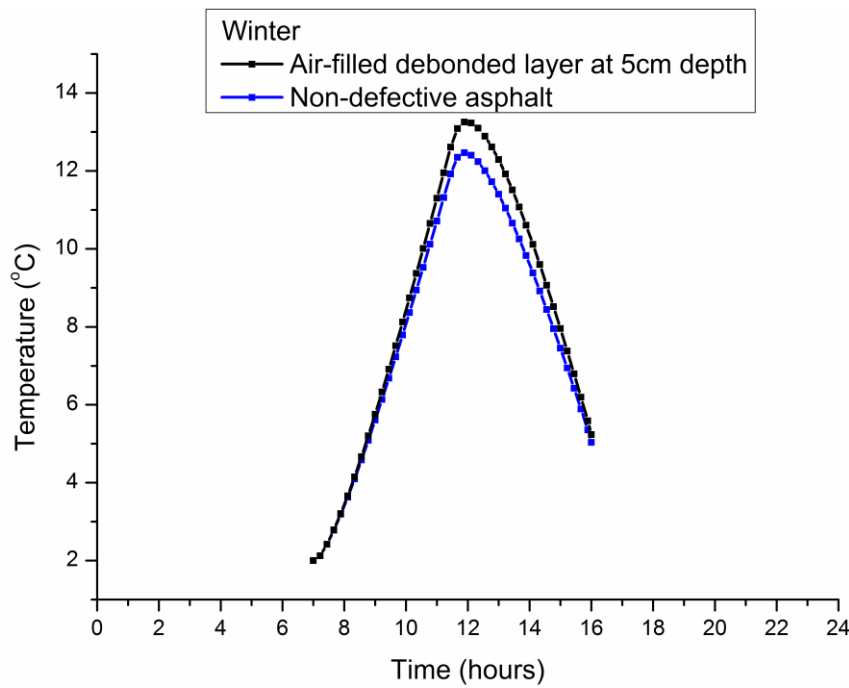


Figure 13: Daily temperature variation at the pavement surface between the non-defective structure and the structure with air-filled debonded layer located at 5cm depth during winter period.

### 4.3 Asphalt with dry (air) or wet (water) debonded layer at 1cm depth

In this section, the effect of dry and wet debonded layers depth location on the temperature differential produced on the pavement surface is examined. In particular, the thermal response of asphalt pavement with debonded layers at 5cm depth, as presented in the previous section, is compared with the corresponding response of the same structure but with the debonded layer located at 1cm depth.

Figures 14 and 15 show the daily variation of TD at the pavement surface between the non-defective structure and the structure with air-filled and water-filled debonded layer respectively located at 1cm depth for all the seasonal periods together. In the pavement containing a air-filled debonded layer maximum TD appears around 12 o'clock noon and a value of about 4°C in summer periods, 3.4°C in autumn/spring periods and 2.1°C in winter periods is calculated. The results show that during all periods sufficient TD is developed on the pavement surface in order for the air-filled debonded layer to be detected during a thermography process. On the other hand, the water-filled debonded layer produces insignificant TD and thus may not be detected by a thermal imager.

Figures 16, 17, and 18 show the daily variation of temperature differential TD at the pavement surface between the non-defective structure and the structure with air-filled debonded layer located either at 5cm depth or at 1cm depth during summer period, spring/autumn period, winter period respectively. The results indicate that maximum TD is diminished when the debonded layer is located deeper in the pavement because near-surface defects affect more the slow rate of heat conduction in the pavement

and thus produce higher temperature differentials on the pavement surface. In particular, when the debonded layer changes location from 5cm to 1cm deep, maximum TD is increased to 4°C from 2°C in summer periods, to 3.4°C from 1.7°C in autumn/spring periods, and to 2.1°C from 0.9°C in winter periods. The results also show that for debonded layers located at 1mm deep maximum TD occurs around 12 o'clock noon and for debonded layers located at 5mm deep maximum TD occurs around one hour later at 13 o'clock noon.

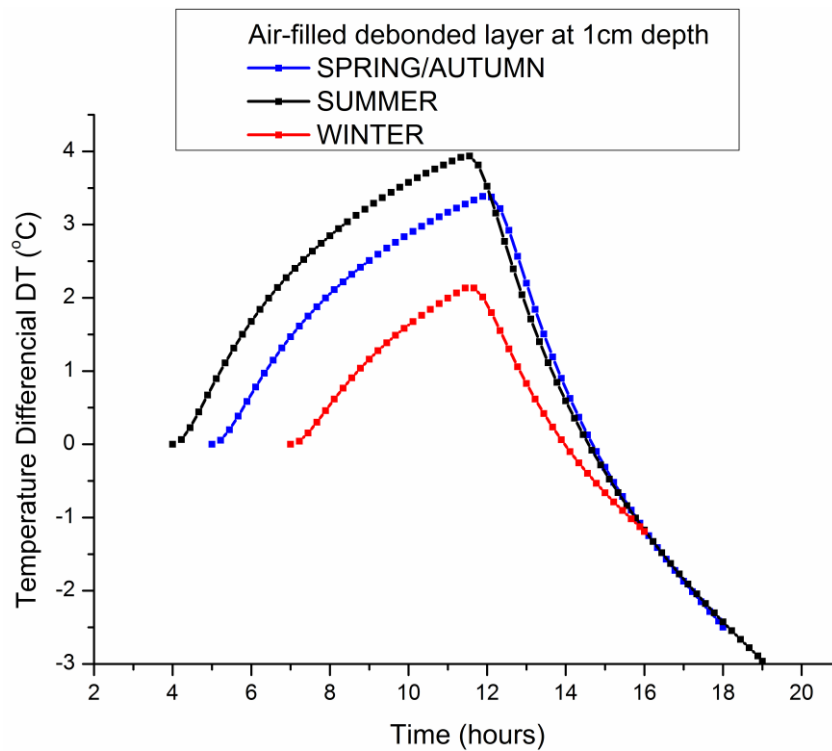


Figure 14: Daily variation of TD at the pavement surface between the non-defective structure and the structure with air-filled debonded layer located at 1cm depth.

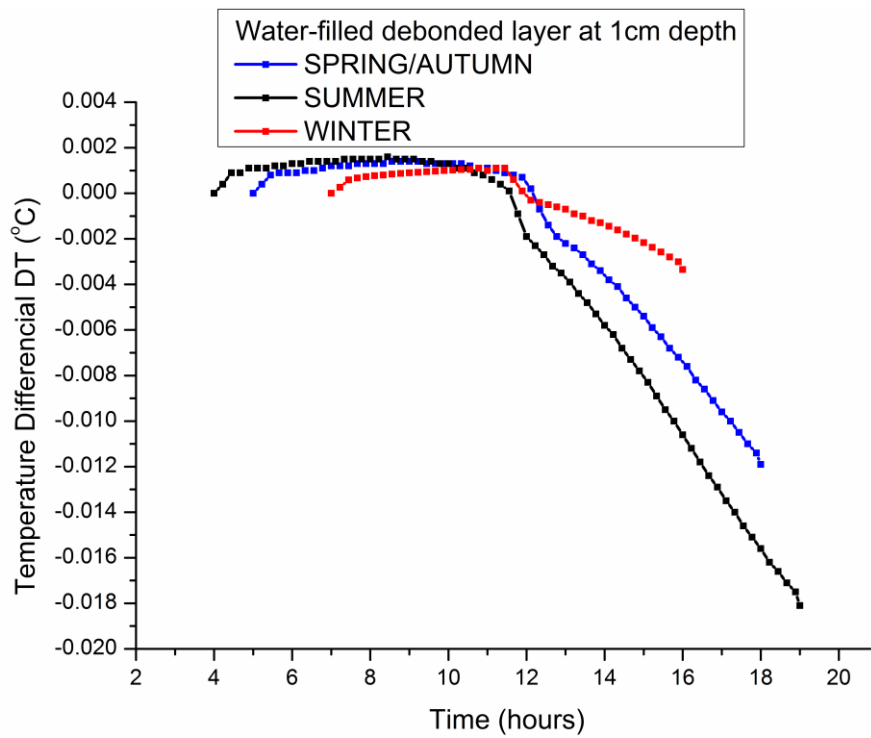


Figure 15: Daily variation of TD at the pavement surface between the non-defective structure and the structure with water-filled debonded layer located at 1cm depth.

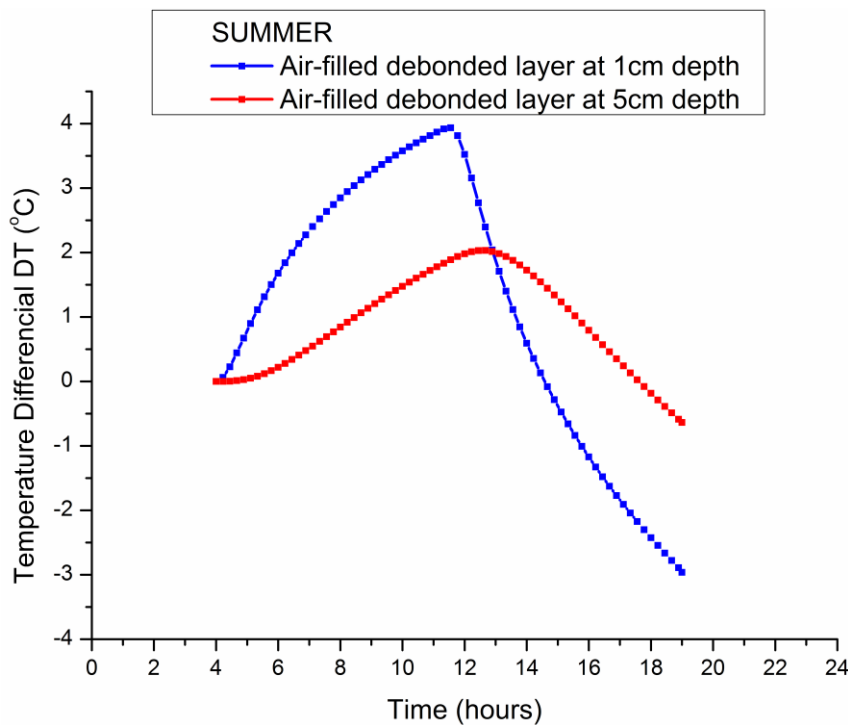


Figure 16: Daily variation of TD at the pavement surface between the non-defective structure and the structure with air-filled debonded layer located at 1cm depth and 5cm depth in summer period.

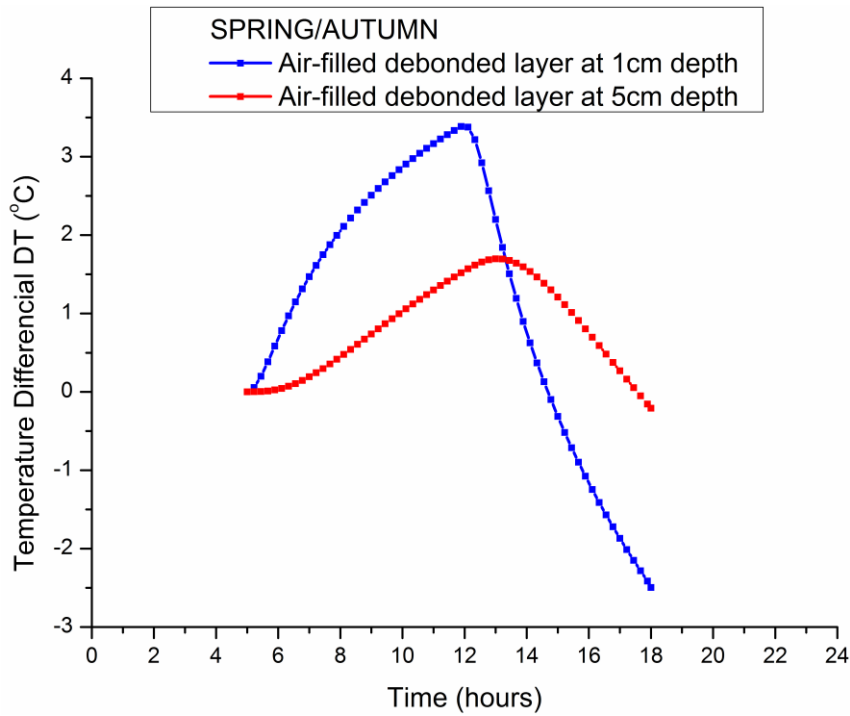


Figure 17: Daily variation of TD at the pavement surface between the non-defective structure and the structure with air-filled debonded layer located at 1cm depth and 5cm depth in autumn/spring period.

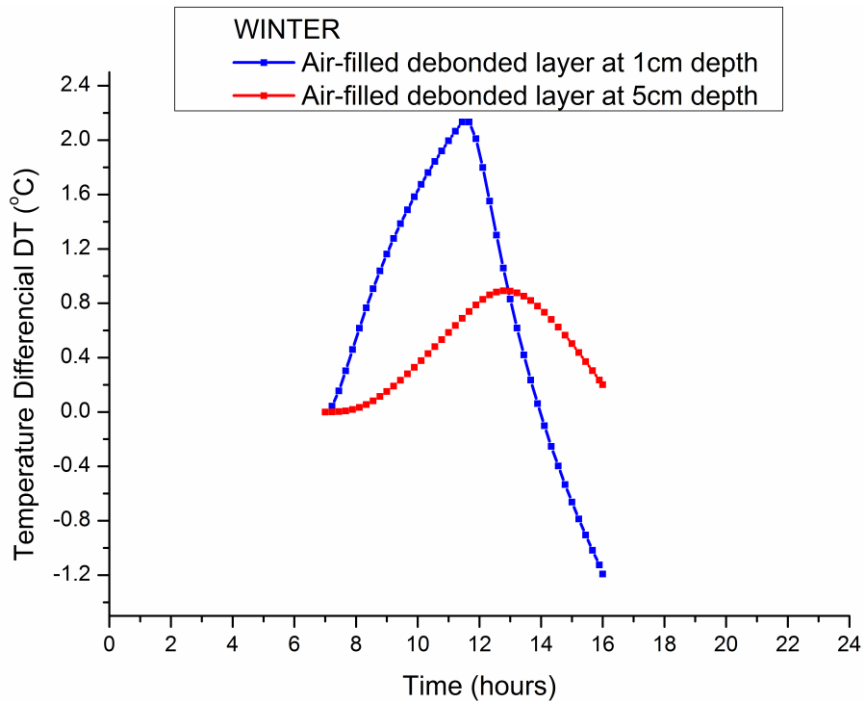


Figure 18: Daily variation of TD at the pavement surface between the non-defective structure and the structure with air-filled debonded layer located at 1cm depth and 5cm depth in winter period.

#### 4.4 Asphalt with partially debonded layer at 1cm depth

In this section, the effect of the debonded layer size on the temperature differential produced on the pavement surface is examined. In particular, the thermal response of asphalt pavement with a fully air-filled debonded layer, as presented in the previous sections, is compared with the corresponding response of the same structure but containing a partially air-filled debonded layer of dimensions 30mm x 30mm x 2mm (length x width x depth) (Figure 19). Both debonded layers are located at 1cm depth.

Figures 20, 22, and 24 show the daily variation of temperature differential TD at the pavement surface between the non-defective structure and the structure containing either a fully or partially air-filled debonded layer located at 1cm depth during summer period, spring/autumn period, winter period respectively. The results indicate that maximum TD is diminished significantly when the size of the debonded layer is half decreased. In particular, when the debonded layer changes dimensions from 60mm x 60mm x 2mm to 30mm x 30mm x 2mm (length x width x depth), maximum TD is decreased to 1.4°C from 4°C in summer periods, to 1.2°C from 3.4°C in autumn/spring periods, and to 0.7°C from 2.1°C in winter periods. The results also show that for both cases maximum DT occurs around 12 o'clock noon.

Figures 21, 23, and 25 show temperature contours at the surface of pavement containing the air-filled partially debonded layer at time of maximum TD during summer period, spring/autumn period, and winter period respectively. It is clearly depicted that in all cases the temperature is raised over the defective regions because defects, which have a lower thermal conductivity than the flawless material, cause a slower rate of heat conduction and thus the surface remains warm longer (Fourier's law).

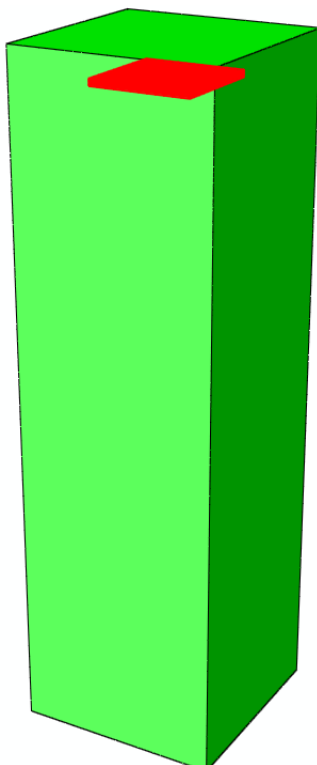


*Figure 19: Model representation of the 3D pavement structure containing partially debonded layer of dimensions 30mm x 30mm x 2mm (length x width x depth) located at 10mm depth.*

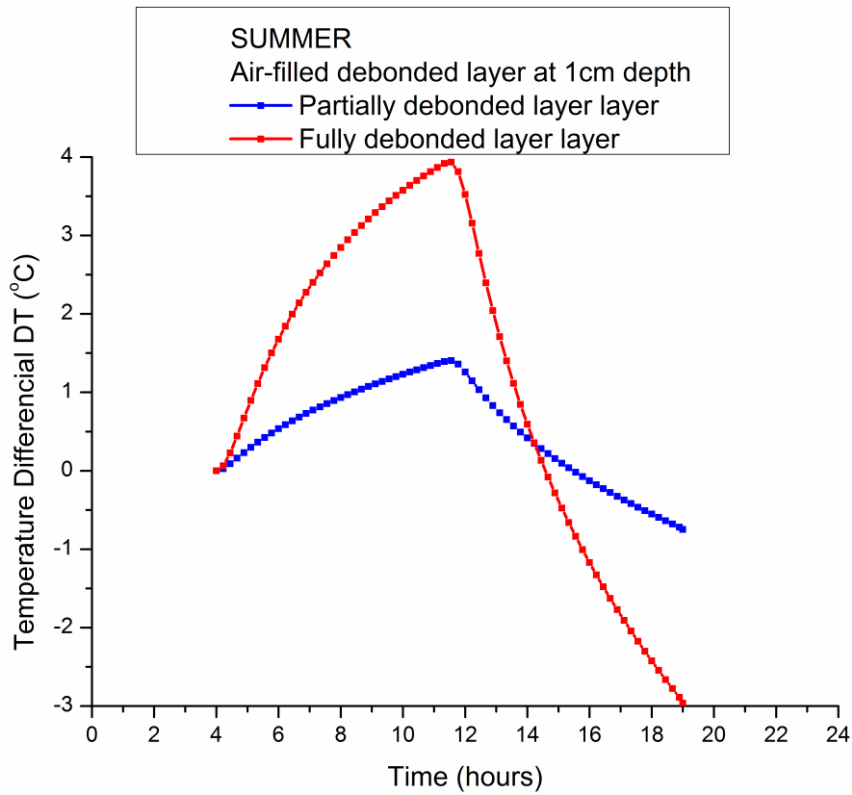


Figure 20: Daily variation of TD at the pavement surface between the non-defective structure and the structure containing either a fully or partially air-filled debonded layer located at 1cm depth during summer period.

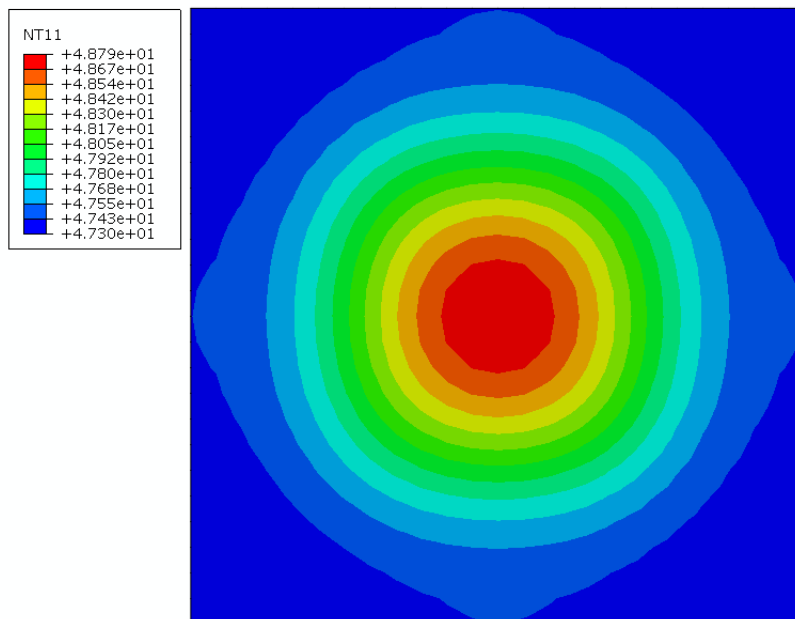


Figure 21: Temperature distribution at the surface of pavement containing air-filled partially debonded layer during summer period at time of maximum TD.

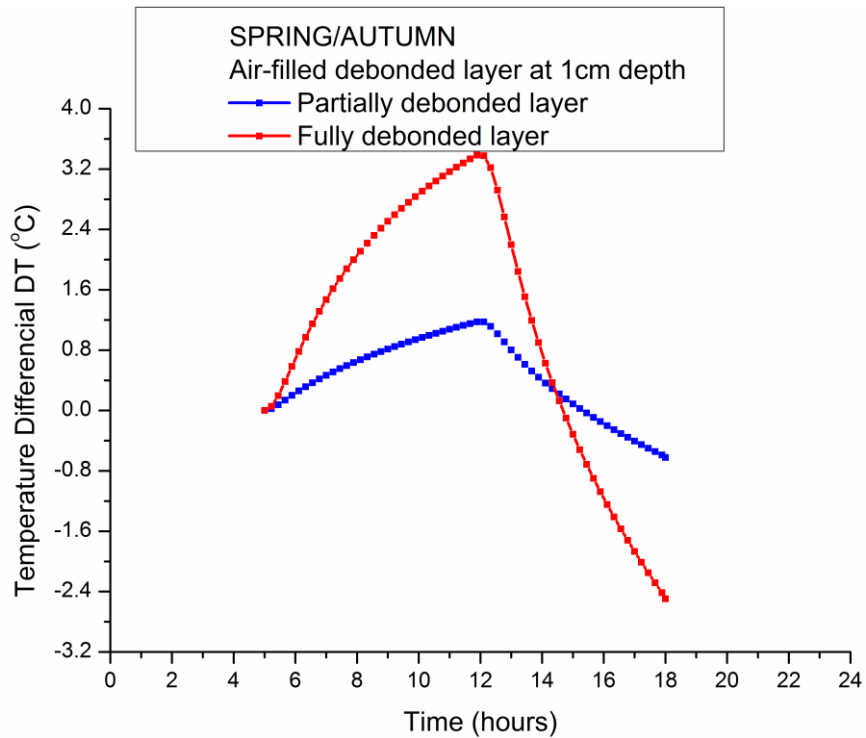


Figure 22: Daily variation of TD at the pavement surface between the non-defective structure and the structure containing either a fully or partially air-filled debonded layer located at 1cm depth during autumn/spring period.

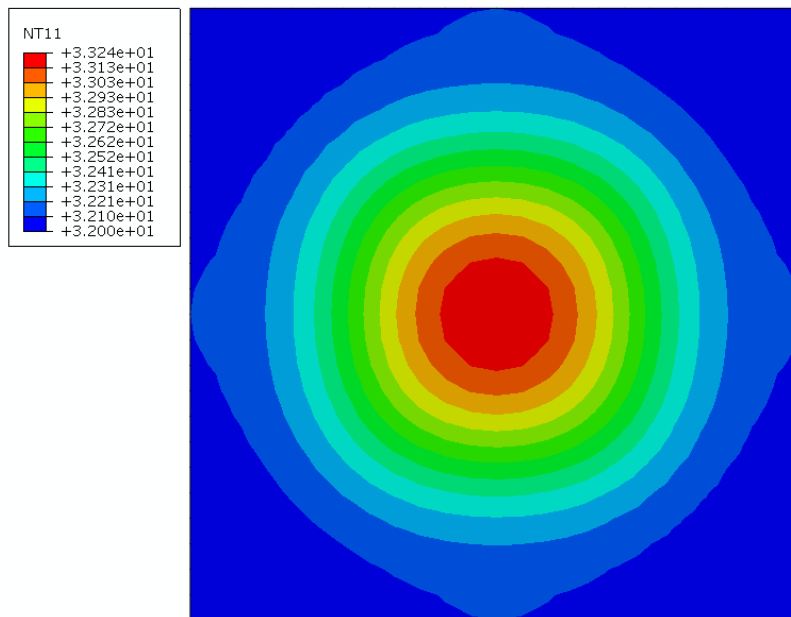


Figure 23: Temperature distribution at the surface of pavement containing air-filled partially debonded layer during autumn/spring period at time of maximum TD.

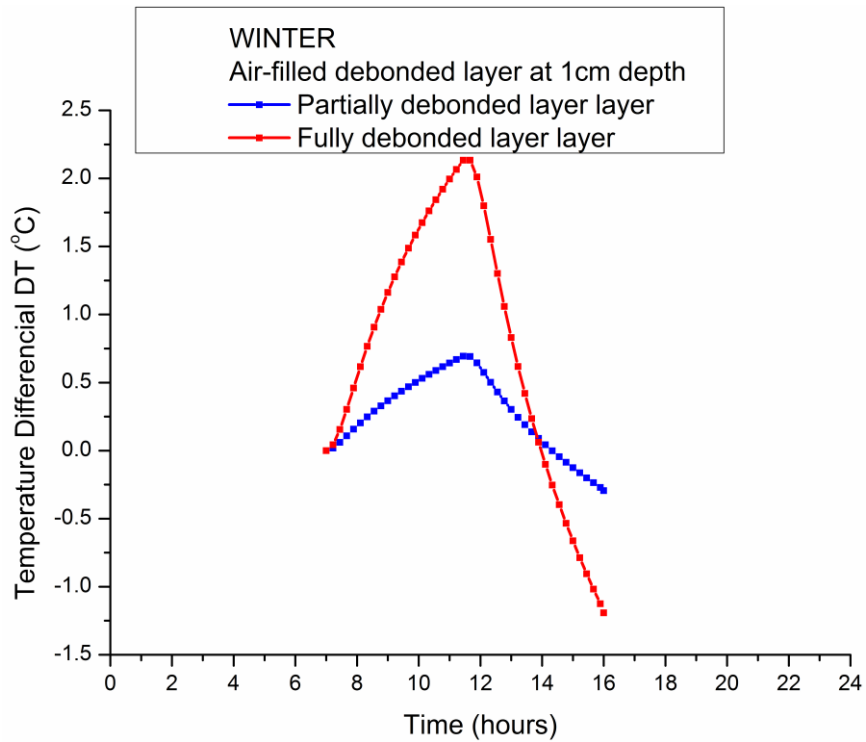


Figure 24: Daily variation of TD at the pavement surface between the non-defective structure and the structure containing either a fully or partially air-filled debonded layer located at 1cm depth during winter period.

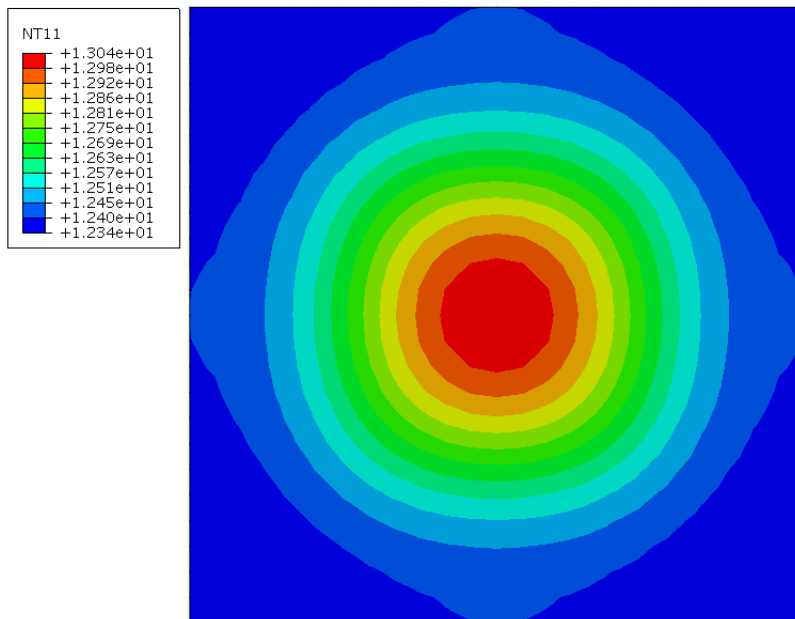


Figure 25: Temperature distribution at the surface of pavement containing air-filled partially debonded layer during winter period at time of maximum TD.

#### 4.5 Asphalt with dry (air) or wet (water) stripped layer at 5cm depth

In this section, the effect of dry and wet stripped layers of thickness 20mm located at 5cm depth on the temperature differential produced on the pavement surface is examined. The dry layer is filled with air whereas the wet layer is filled with 10% water; the properties for stripped asphalt and stripped asphalt with 10% water are shown in Table 1. The rest pavement structure is assumed to be made of intact asphalt.

Figures 26 and 27 show the daily variation of TD at the pavement surface between the non-defective structure and the structure containing either a dry stripped layer or a stripped layer with 10% water located at 5cm depth for all the seasonal periods. In all cases maximum TD appears around 13 o'clock noon. When a dry stripped layer is considered, a TD value of about 0.35°C in summer periods, 0.3°C in autumn/spring periods and 0.15°C in winter periods is calculated. When a wet stripped layer is considered, a TD value of about -0.1°C in summer periods, -0.08°C in autumn/spring periods and -0.04°C in winter periods is calculated.

Figures 28 and 29 show for comparison purposes the daily variation of temperature differential TD at the pavement surface between the non-defective structure and the structure containing either a partially air-filled debonded layer located at 1cm depth or a dry stripped layer located at 5cm depth during summer and spring/autumn periods respectively.

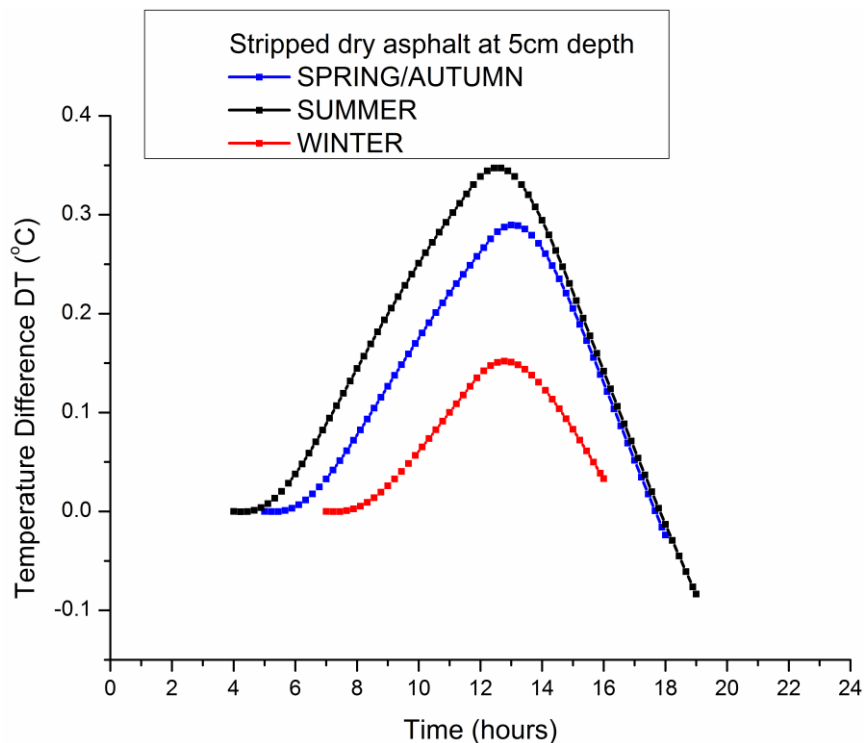


Figure 26: Daily variation of TD at the pavement surface between the non-defective structure and the structure with stripped layer located at 5cm depth.

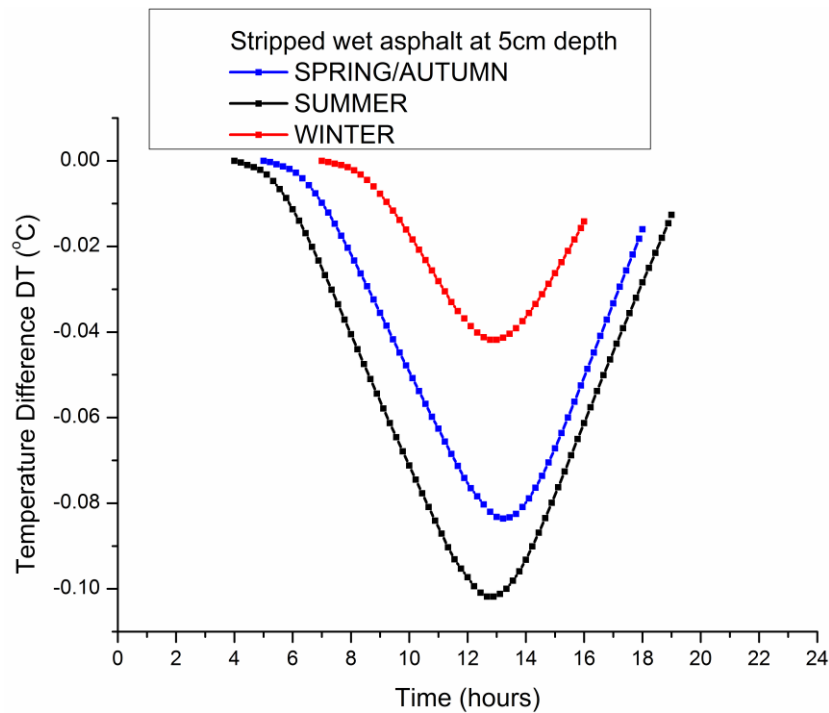


Figure 27: Daily variation of TD at the pavement surface between the non-defective structure and the structure containing a stripped layer with 10% water located at 5cm depth.

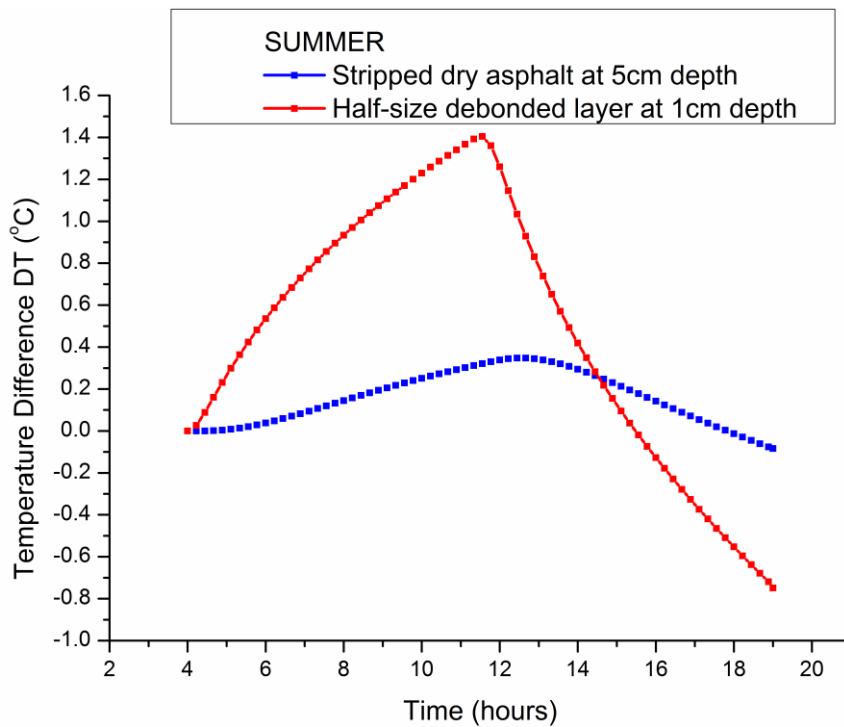


Figure 28: Daily variation of TD at the pavement surface between the non-defective structure and the structure containing either a partially air-filled debonded layer located at 1cm depth or a dry stripped layer located at 5cm depth during summer period.

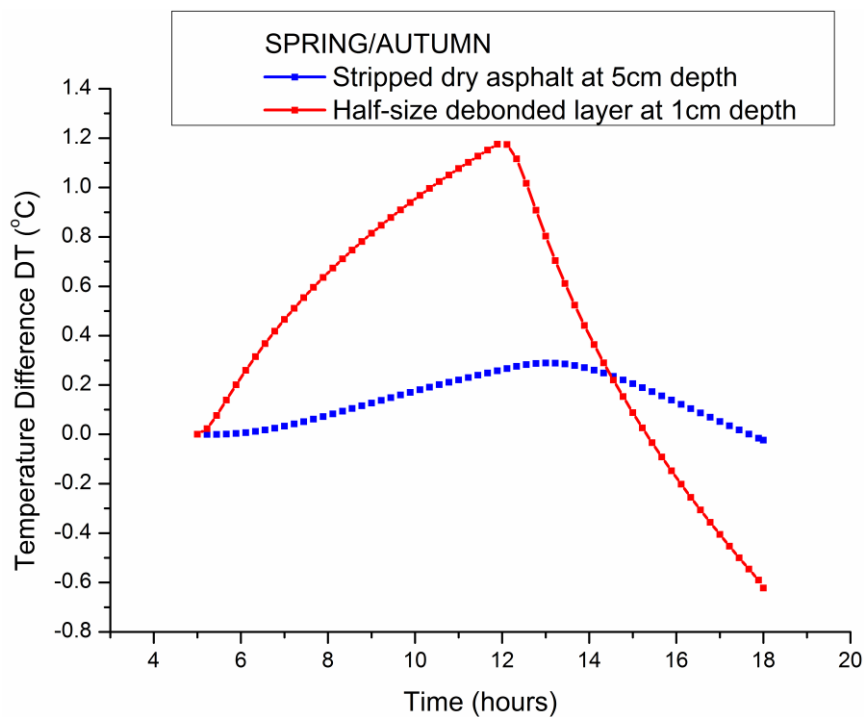


Figure 29: Daily variation of TD at the pavement surface between the non-defective structure and the structure containing either a partially air-filled debonded layer located at 1cm depth or a dry stripped layer located at 5cm depth during autumn/spring period.

#### 4.6 Effect of asphalt thermal conductivity

In this section, the sensitivity of temperature differential on the value of the asphalt thermal conductivity is examined. In particular, we assume that the thermal conductivity of intact asphalt is  $1.5 \text{ W/m}\cdot\text{K}$  instead of  $1.0 \text{ W/m}\cdot\text{K}$ . According to the values presented in Table 1, the thermal conductivities of dry and wet stripped asphalt are considered as 75% and 95% of the value for intact asphalt respectively. The material properties used in the current FE sensitivity study analyses are summarized in Table 3.

Table 3: Thermo-physical properties used in the FE sensitivity study.

| Material                        | Density                  | Thermal Capacity | Thermal Conductivity |
|---------------------------------|--------------------------|------------------|----------------------|
| Intact Asphalt                  | 2300 Kg / m <sup>3</sup> | 1100 J/Kg · K    | 1.5 W / m · K        |
| Stripped Asphalt                | 1800 Kg / m <sup>3</sup> | 1100 J/Kg · K    | 1.125 W / m · K      |
| Stripped Asphalt with 10% water | 2170 Kg / m <sup>3</sup> | 1408 J/Kg · K    | 1.425 W / m · K      |
| Air at 25°C                     | 1.2 Kg / m <sup>3</sup>  | 1006 J/Kg · K    | 0.026 W / m · K      |
| Water at 25°C                   | 1000 Kg / m <sup>3</sup> | 4186 J/Kg · K    | 0.6 W / m · K        |

Figures 30 and 31 show the daily variation of TD at the pavement surface between the non-defective structure and the structure containing either a dry or wet debonded layer located at 1cm depth for different values of asphalt thermal conductivity during spring/autumn period. Figures 32 and 33 show the daily variation of TD at the pavement surface between the non-defective structure and the structure containing either a dry or wet stripped layer located at 5cm depth for different values of asphalt thermal conductivity during spring/autumn period. The results indicate that a more heat conductive asphalt material would cause increase of the temperature differential on the pavement surface. In particular, a change in asphalt thermal conductivity from  $1.5 \text{ W/m}\cdot\text{K}$  to  $1.0 \text{ W/m}\cdot\text{K}$  would cause about  $1^\circ\text{C}$  increase in maximum TD value when the dry debonded layer is contained in the pavement, about  $0.1^\circ\text{C}$  increase in maximum TD value when the wet debonded layer is contained in the pavement, about  $0.02^\circ\text{C}$  increase in maximum TD value when the dry stripped layer is contained in the pavement, and about  $-0.015^\circ\text{C}$  increase in maximum TD value when the wet stripped layer is contained in the pavement.

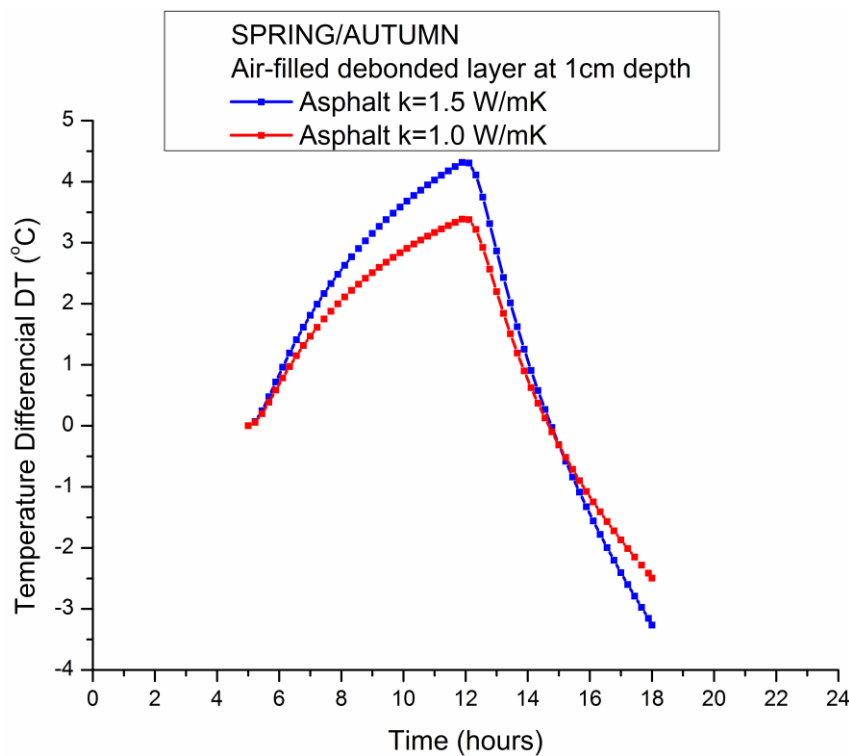


Figure 30: Daily variation of TD at the pavement surface between the non-defective structure and the structure containing a **dry debonded layer** located at 1cm depth for different values of asphalt thermal conductivity during spring/autumn period.

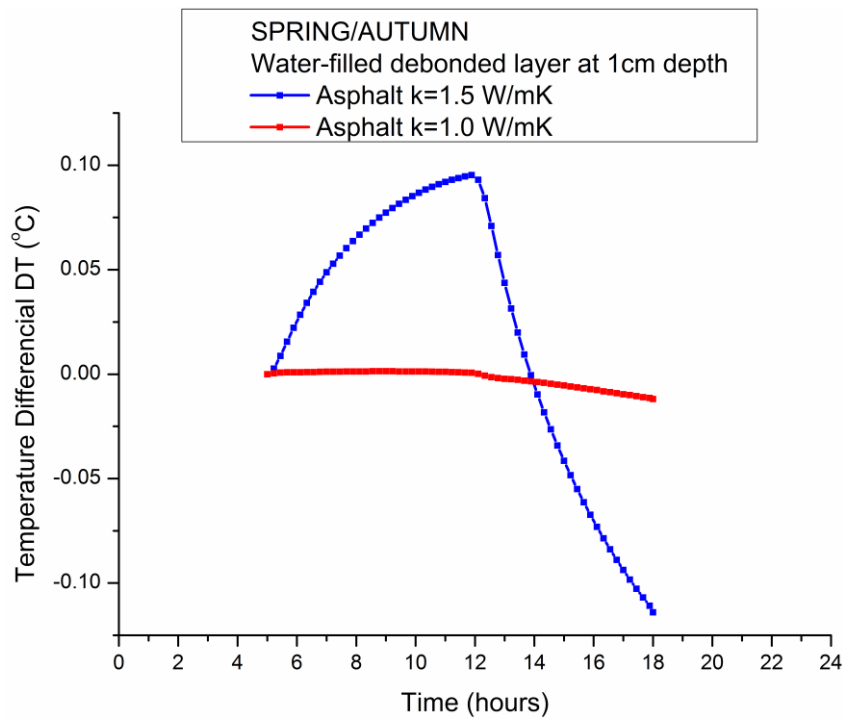


Figure 31: Daily variation of TD at the pavement surface between the non-defective structure and the structure containing a **wet debonded layer** located at 1cm depth for different values of asphalt thermal conductivity during spring/autumn period.

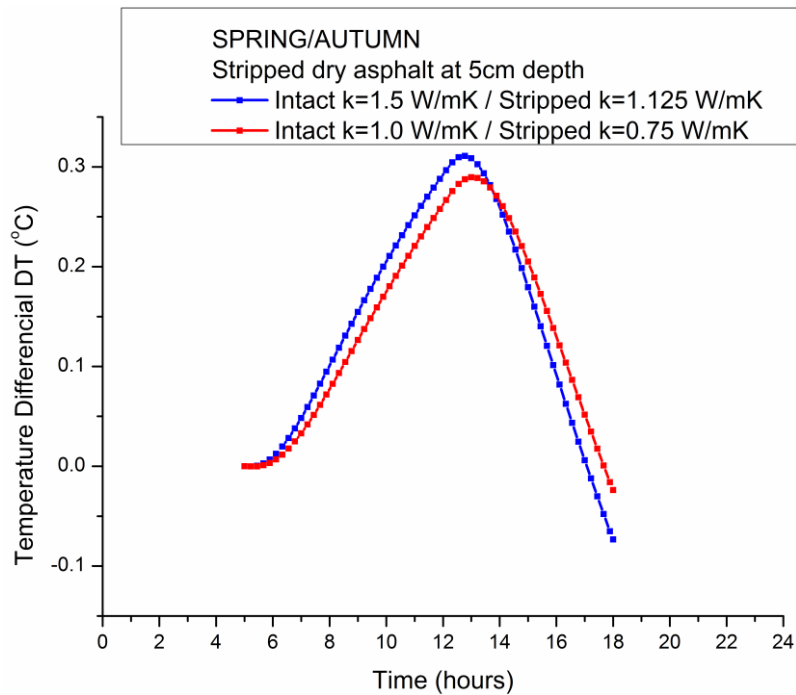


Figure 32: Daily variation of TD at the pavement surface between the non-defective structure and the structure containing a **dry stripped layer** located at 5cm depth for different values of asphalt thermal conductivity during spring/autumn period.

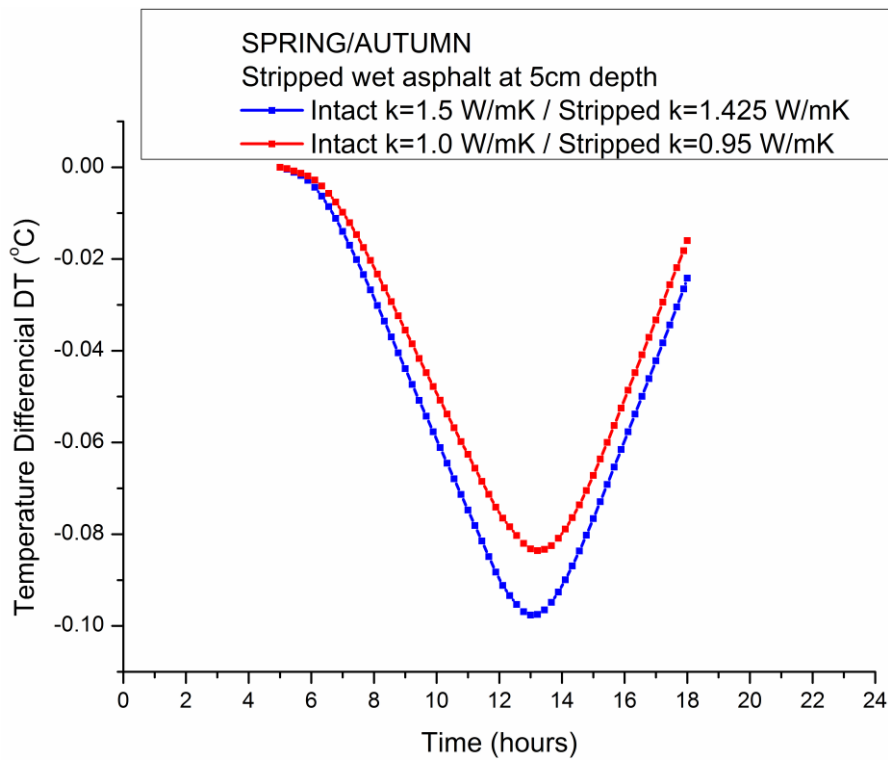


Figure 33: Daily variation of TD at the pavement surface between the non-defective structure and the structure containing a **wet stripped layer** located at 5cm depth for different values of asphalt thermal conductivity during spring/autumn period.

## 5 CONCLUSIONS

3D finite element models were developed to investigate the thermal behavior of asphalt pavement structures containing delaminations (either a debonded or a stripped subsurface layer). The temperature differential (TD) at the pavement surface between defective and intact asphalt was calculated in order to analyze the thermal response of the defects and predict the possibility of identifying them by thermographic techniques. The environmental effects of different seasonal periods (summer, autumn/spring, winter), the pavement condition (dry/wet), as well as the effects of a partially debonded layer, asphalt thermal conductivity, defect depth, on the temperature differential produced on the pavement surface were also examined in the current study.

According to the results the following conclusions can be made:

- (1) An air-filled debonded layer of thickness 2mm located at 5cm depth from the pavement surface, produces sufficient TD between the defective and the intact structure in order to be detected during a thermography process during all the seasonal periods (summer, autumn/spring, winter). If the debonded layer is located closer to the surface (i.e. 1cm depth) the value of TD will be higher and the defect detection will become more evident.
- (2) A water-filled debonded layer of thickness 2mm located at 1cm depth from the pavement surface produces  $DT < 0.1^{\circ}C$  during all the seasonal periods and thus it may not be detected during a thermography process. If the debonded layer is located deeper from the surface, the value of TD will be lower and the defect detection will become more difficult.
- (3) When the size of the air-filled debonded layer of thickness 2mm is half decreased in comparison with the fully air-filled debonded layer, maximum TD significantly diminishes but still sufficient TD is produced in order to detect the defect during a thermography process during all the seasonal periods.
- (4) A dry stripped layer of thickness 20mm located at 5cm depth from the pavement surface, produces sufficient TD between the defective and the intact structure in order to be detected during a thermography process during all the seasonal periods (summer, autumn/spring, winter).
- (5) A wet (10% water) stripped layer of thickness 20mm located at 5cm depth from the pavement surface, produces TD around  $0.1^{\circ}C$  between the defective and the intact structure during summer and spring/autumn periods and thus it may be detected during a thermography process.
- (6) If asphalt's thermal conductivity is  $1.5 W/m \cdot K$  instead of  $1.0 W/m \cdot K$  then maximum TD is increased and defect detection becomes more evident. In that case a water-filled debonded layer of thickness 2mm located at 1cm depth from the pavement surface produces TD around  $0.1^{\circ}C$  during summer and spring/autumn periods and thus it may be detected during a thermography process.
- (7) The ideal time period during a day for thermography inspection is at noon where maximum TD is expected to develop between a defective and a non-defective structure.

## 6 REFERENCES

[1] ABAQUS/Standard, Version 6.12.

[2] Nondestructive testing to identify delaminations between HMA layers Vol.2, Report S2-R06D-RW-2, Chapter 2 “Theoretical Models for Infrared Thermography Technology” pp. 8-10, SHRP2 Renewal Research, Transportation Research Board, US National Academy of Sciences.

[3] Sheeba J.B. and Rohini A.K., “Structural and thermal analysis of asphalt solar collector using finite element method”, Journal of Energy, Vol. 2014, Article ID 602087, 9 pages.

[4] RPB HealTec, Deliverable D1.2 “Preliminary design and selection of appropriate sites for damage assessment and/or inspection”.

[5] Avdelidis N.P., Almond D.P., Dobbinson A., Hawtin B.C., Ibarra-Castanedo C., Maldague X., “Aircraft composites assessment by means of transient thermal NDT”, Progress in Aerospace Sciences, Vol. 40, pp. 143–162, 2004.

[6] Dumoulin J., Ibos L., Ibarra-Castanedo C., Mazioud A., Marchetti M., Maldague X., and Bendada A., “Active infrared thermography applied to defect detection and characterization on asphalt pavement samples: comparison between experiments and numerical simulations”, Journal of Modern Optics, Vol. 57(18), pp. 1759-1769, 2010.